

reducing strongly basic permanganate solutions with  $\text{Na}_2\text{SO}_3$ . The EXAFS spectra were analyzed by using eq 1 with a filtered Fourier transform and fitting procedure in which theoretical phase shift and amplitude functions described by Teo and Lee<sup>11</sup> are used. The absorption edge regions were recorded at small energy steps<sup>18</sup> at room temperature.

Differences in the Mn K near-edge spectrum between polycrystalline  $\text{KMnO}_4$  and aqueous solutions of  $\text{MnO}_4^-$  and  $\text{MnO}_4^{2-}$  are observed. The near-edge regions are displayed in Figure 1 together with their first derivatives. It can be noted that peaks B and C in Figure 1 are considerably broader for the  $\text{MnO}_4^-$  solution than for solid  $\text{KMnO}_4$  while peak A, the  $1s \rightarrow t_2(3d)$  transition, is narrower. Further, a small shift to lower binding energy upon solvation is observed. At the present time, most of this shift is attributed to the instrumentation.<sup>18</sup>

Peaks B and C are consistent with those reported previously<sup>14,19</sup> and can be assigned tentatively to  $1s \rightarrow a_1(4s)$  and  $1s \rightarrow t_2(4p)$  transitions.<sup>17,20</sup> The broadening of these features in solution, particularly peak C (Figure 1), cannot be due to vibrational or collisional broadening. If these mechanisms were pertinent, one would expect a similar, if smaller, effect on the  $1s \rightarrow t_2(3d)$  transition peak A. We propose that the broadening of peaks B and C is due to the formation of virtual resonance (hybridized) states in the dielectric medium. Since the 4p orbitals extend radially from the  $\text{MnO}_4^-$  framework, they can form dynamic "band"-like states with the solvent. This mechanism would broaden the Mn 4p levels of the solid into a resonance state in solution.

Peak D is located 42 and 38 eV above the  $1s \rightarrow t_2(3d)$  transition in  $\text{MnO}_4^-$  and  $\text{MnO}_4^{2-}$ , respectively. These are the resonance states discussed by Kutzler et al.<sup>17</sup> We are presently carrying out calculations<sup>21</sup> for the  $\text{MnO}_4^-$  and  $\text{MnO}_4^{2-}$  ions in order to assign the near-edge spectra quantitatively.

Our EXAFS results for these systems, perhaps the most important information in the present study, are given in Table I together with X-ray crystal data.<sup>22</sup> A typical fit of our data is shown in Figure 2. We can see from Table I that  $\text{MnO}_4^-$  acts as a unit in both solid and solution. The values for the metal-oxygen distances determined by EXAFS and X-ray crystal structure are in close agreement. The difference in the Mn-O bond distance  $\Delta r$  between  $\text{MnO}_4^-$  and  $\text{MnO}_4^{2-}$  in solution<sup>23</sup> is 0.042 Å.

The values for the manganese-oxygen bond distances determined in this study allow one to calculate the activation parameters for the  $\text{MnO}_4^{2-/1-}$ , electron-exchange reaction.<sup>24-26</sup> When formulas based upon a harmonic oscillator model are used,<sup>26</sup> the

Mn-O distance in the transition state is calculated to be 1.644 Å. This corresponds to an inner-sphere reorganization energy of only  $1.6 \pm 0.2$  kcal mol<sup>-1</sup>. The amount of stretching (and compression) of the Mn-O bonds required to reach the transition state are 0.020 and 0.022 Å for  $\text{MnO}_4^-$  and  $\text{MnO}_4^{2-}$ , respectively. These can be compared to the amplitude of the totally symmetric vibration  $\sigma_{\text{vib}}$ . Using 839 and 812 cm<sup>-1</sup> for the symmetric breathing frequency ( $\bar{\nu}$ ) of  $\text{MnO}_4^-$  and  $\text{MnO}_4^{2-}$ <sup>27</sup> and  $\sigma_{\text{vib}}^2 = (h/32\pi^2\mu c\bar{\nu}) \coth(hc\bar{\nu}/2kT)$ ,<sup>28</sup> we obtain  $\sigma_{\text{vib}} = 0.018$  Å for both Mn-O bonds. Thus the symmetric breathing motion at room temperature encompasses almost all of the reorganization necessary. These results can be contrasted with those found for the relatively slow  $\text{Fe}(\text{H}_2\text{O})_6^{2+/3+}$  exchange reaction.<sup>29</sup> For the iron system the difference in Fe-O bond lengths between the two oxidation states is 0.11 Å<sup>1</sup> which results in an inner-sphere reorganization energy of 5 kcal mol<sup>-1</sup>. For this reaction the Fe-O reorganizations are 0.065 and 0.040 Å, and the totally symmetric vibrational amplitude ( $\sigma_{\text{vib}}$ ) are 0.023 and 0.019 Å for  $\text{Fe}(\text{H}_2\text{O})_6^{2+}$  and  $\text{Fe}(\text{H}_2\text{O})_6^{3+}$ , respectively.<sup>1</sup>

**Acknowledgment.** We thank Drs. N. Sutin, M. L. Perlman, J. B. Hastings, J. Davenport, and G. Wendin for discussions. EXAFS spectra were measured at the Stanford Synchrotron Radiation Laboratory, which is supported by the National Science Foundation (under contract DMR77-27489). We also thank SSRL staff for their assistance. Work at Brookhaven National Laboratory was performed under the auspices of the U.S. Department of Energy.

(27) Nakamoto, K. "Infrared and Raman Spectra of Inorganic and Coordination Compounds", 3rd ed.; Wiley: New York, 1978; p 142.

(28) Cyran, S. J. "Molecular Vibration and Mean Square Amplitudes"; Elsevier: Amsterdam, 1968. The definition of  $\mu$  ( $\mu = 16$ ) here is slightly different from that in ref 1. It is also interesting to note that  $(\sum \sigma_{\text{vib}}^2)^{1/2}$  (where  $\sigma_{\text{vib}}$ 's are the vibrational mode discussed in ref 27) are 0.044 and 0.047 Å for  $\text{MnO}_4^-$  and  $\text{MnO}_4^{2-}$ , respectively.

(29) Brunschwig, B. S.; Logan, J.; Newton, M.; Sutin, N. *J. Am. Chem. Soc.* **1980**, *102*, 5898.

### Photodissociation Spectra of Pyridinyl Radical Dimers Detected by Reverse Pulse Polarography. Revised View of the Electrochemistry of Nicotinamide Adenine Dinucleotide

Joshua Hermolin\* and Emilia Kirowa-Eisner\*

Department of Chemistry, Tel-Aviv University  
Ramat-Aviv, Tel-Aviv, Israel

Edward M. Kosower\*

Department of Chemistry, State University of New York  
Stony Brook, New York 11794

Received February 11, 1980

In our studies of 1-alkyl-2-carbomethoxypyridinyl radicals (**2**),<sup>1</sup> we concluded that the absorption spectrum of the major form present in solution (the radical dimer) could be best explained by interpreting the longest wavelength absorption as a  $\pi\sigma \rightarrow \pi\sigma^*$  transition.<sup>1</sup> Although photodissociation of the dimer [(**2**)<sub>2</sub>] to the pyridinyl radical (**2**) can be produced readily by irradiation in thin films at low temperatures or by nanosecond laser pulse irradiation of acetonitrile solutions at 337 nm, it was not possible to obtain excitation spectra for dissociation from these experiments.<sup>1</sup>

Examination of the spectra of 1-alkyl-3-carbomethoxy- and 1-alkyl-3-carbamidopyridinyl radical dimers (3-3) indicated that the longest wavelength absorption bands had (a) a peculiarly low absorption coefficient (in comparison to related 1,4-dihydro-

(18) (a) The resolution of the focused EXAFS beam line with Si (111) crystals is ~3 eV at the Mn K edge (~6.5 keV) (this work). Caution must be used in measuring binding-energy shifts, because of beam instability and monochromator tuning effects.  $\text{KMnO}_4$  has been used as a standard for the calibration of photon energy and resolution of the spectrometer. A width of ~1.5 eV has been obtained for the  $1s \rightarrow 3d$  transition with the SSRL wiggler beam line, compared to ~4 eV reported here. (b) We have observed shifts varying from ~1 eV to a few tenths of an electron volt by running solid and solution samples alternately; more quantitative results which can only be obtained with spectrometers of high resolution are needed to establish the correlation between binding-energy shift and solvation.

(19) The gross feature of the near edge spectrum of  $\text{MnO}_4^-$  has been reported earlier by: (a) Jaklevic, J.; Kirby, J. A.; Klein, M. P.; Robertson, A. S.; Brown, G. S.; and Eisenberger, P. *Solid State Commun.* **1977**, *23*, 679. (b) Rabe, P.; Tolkieln, G.; Werner, A. *J. Phys. C* **1979**, *12*, 1173. No discussion or comparison of the  $\text{KMnO}_4$  solid and solution results are given in these studies, however.

(20) Johnson, K. H. *Adv. Quantum Chem.* **1973**, *7*, 143.

(21) Davenport, J.; Sham, T. K., work in progress.

(22) Palenik, G. J. *Inorg. Chem.* **1967**, *6*, 503, 507.

(23)  $\Delta r$  is 0.03 Å from ref 22 and is an average value. We expect smaller local static disorder in solution due to more spherical screening of the  $\text{MnO}_4^-$  ion by solvent molecules. The estimated error is <0.005 Å. We also obtain  $\Delta r = 0.04 \pm 0.005$  Å by fitting EXAFS data of  $\text{MnO}_4^-$  and  $\text{MnO}_4^{2-}$  with each other.

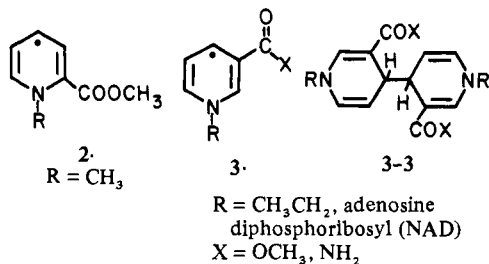
(24) Sutin, N. In "Tunneling in Biological Systems"; Chance, B., DeVault, D. C., Frauenfelder, H., Marcus, R. A., Schrieffer, J. R., Sutin, N., Eds.; Academic Press: New York, 1979 and references therein.

(25) Marcus, R. A. *Annu. Rev. Phys. Chem.* **1966**, *15*, 155.

(26) Sutin, N. *Ann. Rev. Nucl. Sci.* **1962**, *12*, 296 and references therein.

pyridines) and (b) a breadth which seemed too great for a 1,4-dihydropyridine. In addition, the dimer was nonfluorescent, in sharp contrast to the well-known fluorescence of 3-carbamido-1,4-dihydropyridines.<sup>2</sup> Conflicting electrochemical data in the literature added a note of confusion to the study of the redox reactions of 3-carbamido-1-alkylpyridinium ions and the corresponding biologically active NAD<sup>+</sup> and NADP<sup>+</sup> ions: (1) Re-oxidation of the dimer to a pyridinium ion rather than to the expected bipyridylum derivative was noted<sup>3</sup> and explained as being due to a weak bond between the pyridinyl radicals. (2) Slow reduction of the dimer at the second reduction potential for the pyridinium ion led to 1,4-dihydropyridine.<sup>4</sup> (3) The rate constants for dimerization [ $(4 \times 10^2)$ – $(4 \times 10^7)$  M<sup>-1</sup> s<sup>-1</sup>] were inconsistent with those measured by pulse radiolysis ( $1 \times 10^8$  M<sup>-1</sup> s<sup>-1</sup>) (see footnote f, Table I, ref 5). Yet, the dimer was relatively easy to produce and gave no problems on storage.

In light of our results with dimers from **2**·, we considered the



possibility that the longest wavelength absorption of the **3-3** might be a  $\pi\sigma \rightarrow \pi\sigma^*$  transition. Materials with this structure might then be photosensitive and also prone to radical formation through adsorption of the dimer on an electrode surface. We now report the application of the technique of reverse pulse polarography (RPP)<sup>6,7</sup> to the confirmation of these propositions. Furthermore, it is possible to obtain photodissociation spectra for dimers from both **2**· and **3**· radicals (i.e., from **2-2** and **3-3**) which correspond very well to the observed absorption spectra in strong support of the interpretation given for the nature of the electronic transition.<sup>8</sup>

The fundamental experiment involves the measurement of the current flowing at the dropping mercury electrode at various potentials in the absence and presence of light.<sup>9</sup> The RPP

(2) Burnett, R. W.; Underwood, A. L. *Biochemistry* **1966**, *7*, 3328.

(3) Elving, P. Y.; Schmamel, C. O.; Santhanam, K. S. V., *CRC Crit. Rev. Anal. Chem.* **1976**, *6*, 1. See also: Schmamel et al. *J. Am. Chem. Soc.* **1975**, *97*, 5083.

(4) Cunningham, A. J.; Underwood, A. L. *Arch. Biochem. Biophys.* **1966**, *119*, 88–92.

(5) Kosower, E. M.; Teuerstein, A.; Burrows, H. D.; Swallow, A. J. *J. Am. Chem. Soc.* **1978**, *100*, 5185.

(6) Osteryoung, J.; Kirowa-Eisner, E. *Anal. Chem.* **1980**, *52*, 62. Reverse pulse polarography (RPP) has qualitative diagnostic power and combines in one technique the best features of cyclic voltammetry and double potential step chronoamperometry. In the present case, RPP has two advantages: (a) unstable dimers can be prepared in the vicinity of the electrode and their electrochemical properties characterized; (b) irradiation of solutions containing the light-absorbing material (i.e., the dimer) only in the vicinity of the electrode averts a crucial loss of light intensity that would occur if the dimer were distributed throughout the bulk of the solution. Two modes of RPP were used: (a) Constant  $E_{in}$  mode (utilized to obtain the results illustrated in Figure 1). During the first portion of the drop lifetime ( $0.5 \leq t \leq 10$  s), the initial potential is set at a point at which the desired reaction takes place. A single potential pulse ( $0.8 \leq t_p \leq 100$  ms) is then applied. The current flowing during the pulse as a result of the electrochemical activity of the product and intermediates accumulated at  $E_{in}$  is measured. The usual pulse train of normal pulse polarography is used to characterize the initial electrode reaction. (b) Constant  $E_p$  mode (utilized to obtain the results shown in Figure 3). The potential of the pulse is held constant, and the current passing during the pulse is measured as a function of the initial potential, which is changed from drop to drop. The second mode has been named inverse normal pulse polarography (INPP) by Cummings et al. [Cummings, T. E.; Bresnahan, W. T.; Suh, S. Y.; Elving, P. J. *J. Electroanal. Chem.* **1980**, *106*, 71].

(7) RPP has been used in the study of 1-methyl-2-, -3-, and -4-carbomethoxypyridinium ions. Kashti-Kaplan, S.; Hermolin, J.; Kirowa-Eisner, E. *J. Electrochem. Soc.*, in press.

(8) An elegant example of the use of the triple-step potential method in connection with spectroscopic observations on the generation of reactive species has been given by: Faulkner, L. R.; Bard, A. J. In "Electroanalytical Chemistry"; Bard, A. J., Ed.; Marcel Dekker: New York, 1977; Vol. 10, pp 17–20.

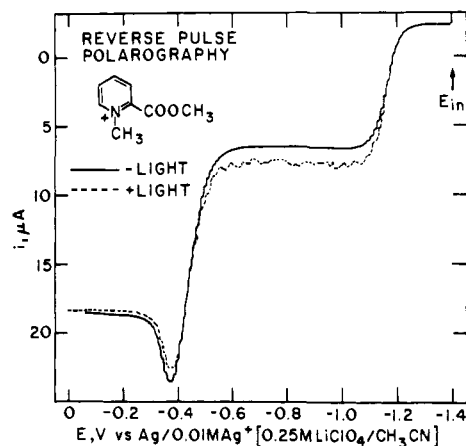


**Figure 1.** Reverse pulse polarograms (constant  $E_{in}$  mode) of 1-methyl-2-carbomethoxy-4-methylpyridinium radical dimer (**2-2**) perchlorate (0.95 mM) in 0.25 M LiClO<sub>4</sub>-CH<sub>3</sub>CN. Without light, —; with light, - - (irradiation with pulsed N<sub>2</sub> laser).  $E_{in}$  (-1.4 V) vs. Ag/0.01 M Ag<sup>+</sup> (CH<sub>3</sub>CN) ( $t = 0.5$  s);  $E_p$  plotted on the X axis ( $t_p = 1.7$  ms).

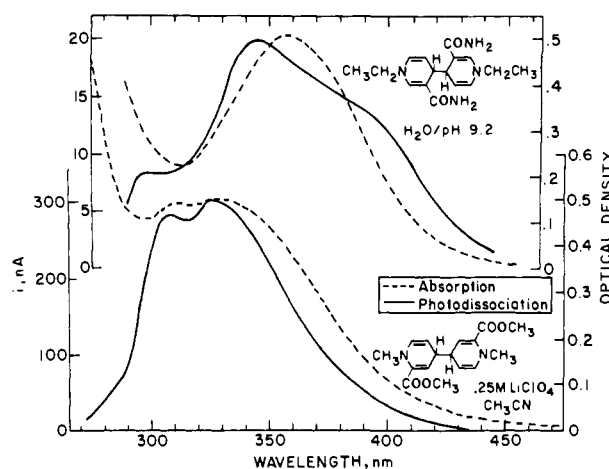


**Figure 2.** Photodissociation (—) and absorption (---) spectra of (upper curves and axes) 1-ethyl-3-carbamidopyridinyl radical dimer (**3-3**) and (lower curves and axes) 1-methyl-2-carbomethoxy-4-methylpyridinyl radical dimer (**2-2**). The photodissociation curves were obtained by plotting the measurements of the reverse pulse current of the radical oxidation made under irradiation after subtracting the dark current obtained in the absence of irradiation. Both dimers were generated in the vicinity of the electrode by RPP as follows: (**2-2**): 1-methyl-2-carbomethoxy-4-methylpyridinium (**2<sup>+</sup>**) perchlorate (0.6 mM) in 0.25 M LiClO<sub>4</sub>-CH<sub>3</sub>CN.  $E_{in}$  (-1.3 V) vs. Ag/0.01 M Ag<sup>+</sup>(CH<sub>3</sub>CN) ( $t = 2$  s);  $E_p = -1.0$  V ( $t_p = 1.7$  ms). (**3-3**): 1-ethyl-3-carbamidopyridinium (**3<sup>+</sup>**) perchlorate in 0.25 M LiClO<sub>4</sub>-aqueous NaHCO<sub>3</sub>-K<sub>2</sub>CO<sub>3</sub>, pH 9.2 buffer.  $E_{in}$  (-1.3 V) vs. SCE ( $t = 2$  s);  $E_p = -1.0$  V ( $t_p = 0.8$  ms).

technique allowed the preparation of the dimer at the first reduction potential for the pyridinium ion used ( $t =$  up to 10 s), followed by a jump to potentials ( $t_p = 0.8$ –90 ms) suitable for oxidation of the pyridinyl radicals or the pyridinyl radical dimers.

RPP was applied to 1-methyl-2-carbomethoxy-4-methylpyridinium ion (**2<sup>+</sup>**) to establish the validity of the approach. The anodic currents recorded in Figure 1 correspond to the oxidation of species formed at the initial potential. ( $E_{in}$  is maintained at the plateau of the first reduction wave of **2<sup>+</sup>**, a potential at which radicals are produced and rapidly equilibrate with the corresponding dimers.<sup>7</sup> The radicals are oxidized at  $E_{1/2} = -1.166$  V and the dimers at  $E_{1/2} = -0.48$  V. The limiting currents at each of the two oxidation waves reflect the amounts of radical and dimer, respectively, present at the electrode surface as a result of the reduction at  $E_{in}$  immediately prior to the switching of the potential to those at

(9) Although different light sources were used (200-W Hg lamp, 150-W Xe lamp with a monochromator, pulsed N<sub>2</sub> laser (100 kW/cm<sup>2</sup> per pulse, 10–30 Hz, 1.5-ns pulse), no effect was noted on the shape and position of a usual polarogram of the pyridinium ions used, including NAD<sup>+</sup>.

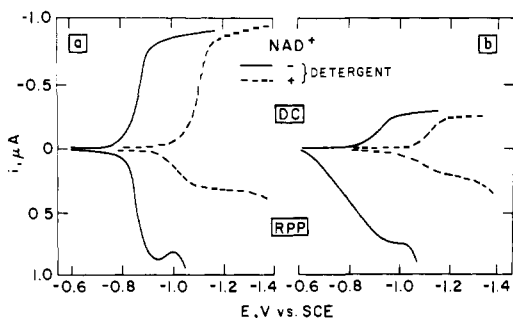


**Figure 3.** Direct current (DC) polarograms and reverse pulse polarograms (RPP) (constant  $E_p$  mode) of  $\beta$ -nicotinamide adenine dinucleotide ( $NAD^+$ ). RPP:  $E_{in}$  plotted on the X axis ( $t = 0.5$  s);  $E_p = -0.6$  V (in absence of detergent),  $E_p = -0.8$  V (in presence of 0.006% detergent, Triton X-100) ( $t_p = 0.8$  ms). (a)  $\beta$ - $NAD^+$  (0.76 mM), 0.25 M Li-ClO<sub>4</sub>-aqueous NaHCO<sub>3</sub>-K<sub>2</sub>CO<sub>3</sub>, pH 9.2 buffer. (b)  $\beta$ - $NAD^+$  (0.76 mM) is 75% reduced to dimer electrochemically, making the resulting solution ca. 0.28 mM  $NAD\cdot$  dimer and ca. 0.19 mM  $NAD^+$ .

which the current was recorded. It may be seen from the results shown in Figure 1 that irradiating the electrode during the RPP experiment increases the current measured at the potential for radical oxidation, i.e., that light causes the conversion of dimers into radicals detectable within the diffusion layer. Scanning the wavelength range from 270 to 600 nm produces the photodissociation spectrum shown in the lower part of Figure 2 in which comparison is made to the independently determined absorption curve for the dimer.<sup>1</sup>

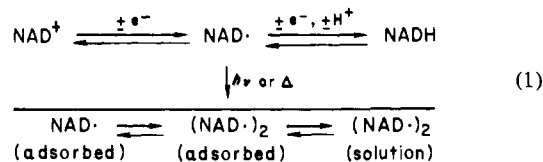
Irradiation of a solution of 1-ethyl-3-carbamidopyridinium ion in lithium perchlorate-carbonate buffer, pH 9.2, produces a small but well-defined increase in the current at the oxidation potential for the 3-substituted pyridinyl radicals. The wavelength dependence of the current increase bears a close resemblance to the absorption spectrum of the dimer as shown in the upper part of Figure 2 and is thus identified as a photodissociation spectrum of the dimer. Parallel observations have been made for 1-ethyl-3-carbomethoxypyridinium perchlorate in 0.25 M Li-ClO<sub>4</sub>/CH<sub>3</sub>CN, showing that the solvent does not alter the close resemblance between the photodissociation spectrum and the absorption spectrum of the pyridinyl radical dimer.

Irradiation with an N<sub>2</sub> pulse laser (100 kW/cm<sup>2</sup> per pulse, pulse width ca. 1.5 ns, 10-30 Hz) at 337 nm of  $NAD\cdot$  dimer (produced from  $NAD^+$ <sup>10</sup> in aqueous buffer, pH 9.2, during RPP,  $E_{in} = 1.0$  V vs. SCE,  $t = 2$  s), gave rise to a transient current of radical oxidation in the course of a  $t_p$  ( $E_p = -0.6$  V,  $t_p = 2$  ms), the current being detected by an oscilloscope. The maximum current of the transient was 7  $\mu$ A (a value limited by the rise time of the potentiostat). The transient decayed during 250-300  $\mu$ s to the value of the current (2  $\mu$ A) flowing in the absence of irradiation. (Transients were observed also for 2<sup>+</sup> and (CONH<sub>2</sub>)<sub>3</sub><sup>+</sup>). We were unable, for lack of a suitable dye laser and the limitations imposed by the small magnitude of the current increase found, to obtain a reliable photodissociation spectrum for  $NAD\cdot$  dimer. Other experiments, however, show that  $NAD\cdot$  radicals form easily on the electrode surface from adsorbed  $NAD\cdot$  dimer. Polarography of  $NAD^+$  in aqueous buffer yields a current vs. voltage curve of the expected shape and position. However, RPP of such a "sample" reveals the presence of a substantial amount of adsorbed substance which has the oxidative properties of the  $NAD\cdot$  radical. Addition of a detergent to the solution does not affect the polarographic wave height but sharply diminishes the amount of adsorbed radical,<sup>3</sup> as observed by the RPP  $E_p$ -constant mode technique (termed INPP by Cummings et al.<sup>6</sup>), seen in Figure 3a. (-0.6 V).

The amount of radical generated at different initial potentials (-0.6 to -1.4 V) is measured by the current flowing during a pulse applied in the potential range for the oxidation of the radical (-0.6 V). (The effect of surfactants such as tetraethylammonium ion

on the adsorption of  $NAD^+$  and its reduction products have been discussed by Elving and co-workers.<sup>3</sup>) If 75% of the  $NAD^+$  is reduced electrochemically to the  $NAD\cdot$  dimer, the polarographic current is correspondingly reduced as expected, but the quantity of adsorbed radicals detected by RPP remains unexpectedly high in concentration. Addition of detergent to the "prereduced" solution again diminishes the  $NAD\cdot$  radical present on the surface, as illustrated in Figure 3b.

Many of the apparently conflicting results concerning the electrochemistry of  $NAD^+$ , as summarized by Elving,<sup>3</sup> can be understood as the result of photodissociation or thermal dissociation of  $NAD\cdot$  dimer, either adsorbed or in solution. The scheme for electrochemical  $NAD^+$  reduction should thus be written as in eq 1. The one-electron reduction potential estimated for  $NAD^+$



from pulse radiolysis results (-1.19 V vs. SCE) should not be subject to the complications introduced by adsorption,<sup>11</sup> and is in reasonable agreement with the result estimated for zero dimer interference on the basis of present work in detergent solution. (See Figure 3). Stabilization of  $NAD\cdot$  radicals by combination with the coenzyme binding sites of enzymes has been demonstrated by using pulse radiolysis to generate the  $NAD\cdot$  radicals.<sup>12</sup>

The present results contribute strongly to our understanding of the nature of the electronic transitions in unstable radical dimers and provide an important element of knowledge for the understanding of the behavior of  $NAD\cdot$  radicals. The RPP technique seems to be a convenient and useful way of obtaining photodissociation spectra of many radical dimers.

(11) Farrington, J. A.; Land, E. J.; Swallow, A. J. *Biochim. Biophys. Acta* **1980**, *590*, 273-276.

(12) Bielski, B. H. J.; Chan, P. C. *J. Am. Chem. Soc.* **1980**, *102*, 1713-1716.

### Metal-Metal Interactions in Binuclear Rhodium Isocyanide Complexes. Polarized Single-Crystal Spectroscopic Studies of the Lowest Triplet $\leftarrow$ Singlet System in Tetrakis(1,3-diisocyanopropane)dirhodium(2+)

Steven F. Rice and Harry B. Gray\*

Contribution No. 6325  
from the Arthur Amos Noyes Laboratory  
California Institute of Technology  
Pasadena, California 91125

Received October 10, 1980

The description of the electronic structures of systems containing relatively weak metal-metal bonds between square planar d<sup>8</sup> units is a problem that has received much attention.<sup>1</sup> Our own efforts in this area have centered around several well-defined rhodium(I) isocyanide oligomers, the prototypal complex being Rh<sub>2</sub>b<sub>4</sub><sup>2+</sup> (b = 1,3-diisocyanopropane).<sup>2,3</sup> The lowest triplet excited state of Rh<sub>2</sub>b<sub>4</sub><sup>2+</sup> is of particular interest, owing to its rich photophysical and photochemical properties.<sup>4-6</sup> We have now obtained the

(1) Miller, J. S.; Epstein, A. J. *Prog. Inorg. Chem.* **1976**, *20*, 1.

(2) Lewis, N. S.; Mann, K. R.; Gordon, J. G., II; Gray, H. B. *J. Am. Chem. Soc.* **1976**, *98*, 746.

(3) Mann, K. R.; Thich, J. A.; Bell, R. A.; Coyle, C. L.; Gray, H. B. *Inorg. Chem.* **1980**, *19*, 2462.

(10)  $\beta$ - $NAD^+$  supplied by Sigma-Aldrich was utilized in all experiments.